Title	Absorption characteristics of SI adatoms on the Si(100) and Si(110) surfaces
Author(s)	Toh C. P. and Khoo G. S.
Source	High-Performance Computing Conference '94, 29 – 30 September 1994, Singapore

ADSORPTION CHARACTERISTICS OF
SI ADATOMS ON THE SI(1OO) AND SI(110) SURFACES

Toh C. P.
&
Khoo G. S.

ADSORPTION CHARACTERISTICS OF SI ADATOMS ON THE SI(100) AND SI(110) SURFACES

C.P. TOH
Department of Physics
National University of Singapore
Lower Kent Ridge Road
Singapore 0511

and

G.S. KHOO
Division of Physics
School of Science (National Institute of Education)
Nanyang Technological University
469 Bukit Timah Road
Singapore 1025

ABSTRACT

We have employed a semiempirical molecular orbital method and a modified form of the Stillinger-Weber potential to investigate the characteristics of adsorption and diffusion of Si adatoms on the Si(110) and Si(100) surfaces. Our results for Si(110) indicate that the diffusion of the Si adatom is anisotropic along a low-energy zigzag path directly above the surface atomic zigzag chain. The activation energy for the Si adatom to diffuse along this zigzag path on the Si(110) surface is 0.054 eV, suggesting that the Si adatom is highly mobile on Si(110). For the Si(100) surface, the activation energy is about 0.33 eV with the direction of easy diffusion being parallel and to the side of the dimer rows on the fully relaxed Si(100) 2X1 surface.

1. INTRODUCTION

Though Si is one of the most widely studied materials due to its pre-eminence and long tradition in the semiconductor industry, knowledge is still deficient with regards to adsorption of intrinsic and extrinsic defects on one of its surfaces, the Si(110) [1-6]. Especially intriguing is the long-range ordered "16X2" structure first suggested by Yamamoto et al. [7], which has been confirmed to be a surface structure appearing only on the clean Si(110) surface [8]. Several models have been proposed to explain this "16X2" structure. Ampo et al. [3] suggested that this structure can be represented by an alternation of steps along the [110] direction. On the other hand, Nesterenko and Shkrebtii [4] attempted to explain it in terms of the "dimer-adatom" model, reminiscent of the 'dimer-adatom-stacking fault" model suggested for the Si(111)-(7X7) face [9] and also due to thesimilarity of the common chainlike structures of the ideal Si(110) and the ii-bonded chain model of Si(111)-(2X1) [10].

Recently, STM observations of these "16X2" structures led to the conclusion that they cannot be explained in terms of the vicinal surface model [7]. In these STM experiments, bright and faint zigzag chains consisting of spheres, and the repetition of the upper and the lower layers with a height difference of 2 A were observed. The spheres are believed to be Si adatoms and the zigzag chains illustrate the arrangement of the Si adatoms on the clean Si(110) surface [8]. It should be noted however, that the adatom bonding and positions on Si(110) are still not clearly understood, although the basic building block for the "16X2" structure, whose chain-like structure is also zigzag in nature, is believed to be a Si adatom. Hence, one objective of this work is to determine the nature of the interactionbetween the Si adatom and the Si(110)

surface in terms of its diffusion and chemisorption site.

For the Si(100)2X1 surface, very little is still known about the motion of a single Si atom on the surface as it is virtually impossible to obtain the diffusion coefficient directly. A variety of experimental techniques are available for the examination of surface diffusion. Unfortunately, these techniques are not easily applicable to our Si systems. Recently, several theoretical groups [11-14] have shown that surface migration is faster along the substrate dimer rows than perpendicular to them. STM experiments [15,16] have since been performed to verify these results. Even then, it is still uncertain as to which path along the dimer row the adatom will take, whether it is on top or to the side of the row. In this paper, we also report on a study of the mobility of a Si atom on the Si(100) 2X1 surface.

2. THEORY

We use a combination of two approaches: a semiempirical self-consistent molecular orbital theory, the Complete Neglect of Differential Overlap (CNDO) method [17] and a modified form of the Stillinger-Weber (SW) potential as proposed by van der Eerden et al. [18]. The original SW potential [19] describes well the stability of the diamond structure, the density increase upon melting, the latent heat of sublimation, the lattice constant, the bulk modulus and the bulk melting point. It also predicts correctly some of the properties of the (100) surface. However, the values obtained for the elasticity tensor do not agree well with literature values. We believe that the modified SW potential is more adequate for surface simulations as it has been fitted to reproduce well the elastic constants.

With this potential, we can then proceed to locate the various adsorption sites and energy barriers between sites by standard Monte Carlo (MC) simulation.

For the CNDO method, we implement the MOSES code [20] in our calculations. Previously, this method has also been used to investigate desorption induced by electronic transitions (DIET) processes on semiconductor surfaces [21-24], as well as
the diffusion and adsorption properties of K and Al on the stepped and unstepped GaAs(110) [25] and GaP(110) [26] surfaces respectively.

3. METHODOLOGY

The various adsorption sites of a Si atom on the Si surface are obtained firstly via the Monte Carlo simulated annealing. The sample consists of a stack of 10 layers of 14 X 6 atoms each with a vacuum spacing of about 8 A above the surface. In the lateral directions, we have periodic boundary conditions. The adatom is placed in a fixed horizontal position about 1 A above the slab and the entire system is allowed to relax to its minimum-energy configuration. This is achieved by first equilibrating the system at 300 K and then decreasing the temperature by 5 K for every 10 Monte Carlo steps, as suggested by Wilson, Todd and Sutton [27] until near absolute zero. After cooling, the system is again equilibrated until a minimum energy is attained. This is repeated for a grid of lateral positions within the area shown by the dotted line in Fig. 1a. For each position, the
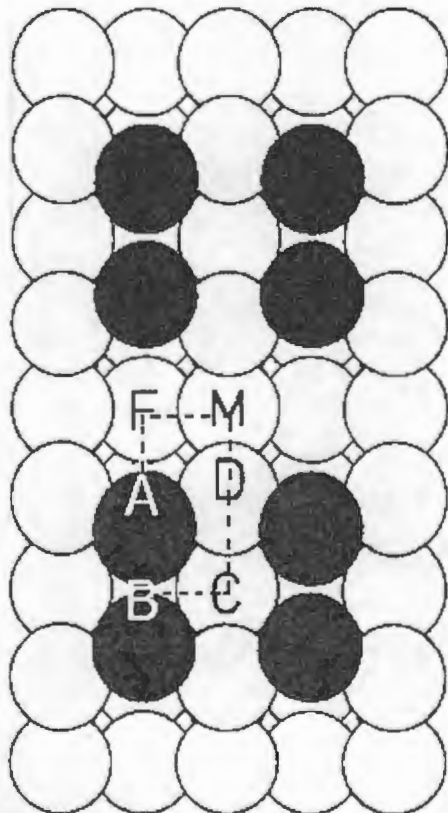
various energies (two-body, three-body, etc.), adatom height, and nearest dimer bond length are noted. All energy values are relative to the fully relaxed clean Si surfaces. From the results, we can deduce the most probable path for diffusion of a single Si adatom as well as the activation energy for diffusion. For the second method using the MOSES code, we simulate the Si surface by using an 84-atom surface cluster, which has previously been used in our studies on DIET phenomena [21-24] as well as the metal-semiconductor surface interaction [25,26], details of which have been reported elsewhere [21-26]. The parameters for Si are those determined by Harker and Larkins [28], and for the perfect Si surfaces, total energy calculations are performed for the Si adatom at various locations along the three traverses P, Q and R within the rectangular grid ABCD on the Si surface (see Fig. 1b). At each site, the Si adatom is relaxed perpendicularly to the surface to obtain the lowest energy. By repeating the minimum energy values obtained at these sites within the rectangular grid
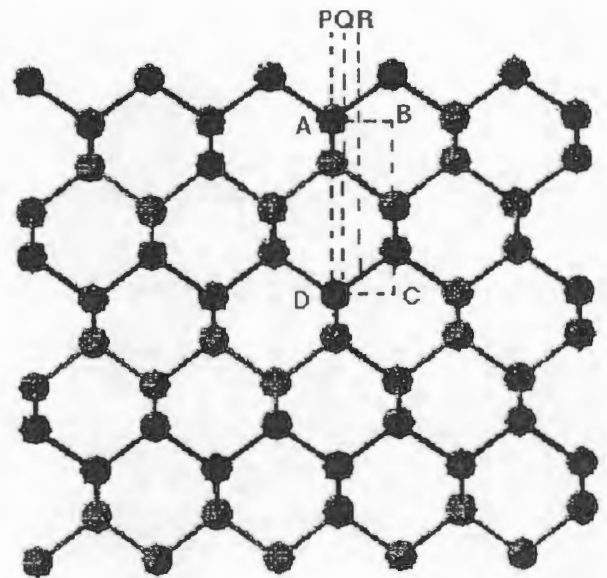

Fig. 1b. The Si adatom is placed at various sites along the traverses P, Q, and R within the rectangular grid ABCD on the Si(110) surface. The surface atoms are represented as darker circles. At each site, the minimum energy is determined by relaxing the adatom perpendicularly to the surface.

ABCD along the whole surface, the total energy surface for a Si adatom on the Si surfaces can be constructed.

4. RESULTS AND DISCUSSIONS

A. Si Adatom on Si(100)-2X1 surface

In Table 1, we list the energies of the sites shown in Fig. 1a.

Fig. 1a. The sites labelled F, A, B and D are the adsorption sites for a Si adatom on the Si(100)-2X1 surface. M and C correspond to local maxima.

298

Table 1(a) Energetic of a Si adatom on Si(001) - 2 xsurface

Site	Total Energy E (eV)	Two-point Energy (eV)	Correction Three-point Energy (eV)	Repulsive Three-point Energy (eV)
B	-2.70	-1.03	-1.15	-0.52
A	-2.27	-1.98	-0.31	0.02
F	-3.16	-3.46	-0.44	0.74
D	-2.46	-3.76	-0.34	1.64
M[a]	-1.23	-3.88	-0.76	3.41
C[a]	-1.57	-5.21	-0.33	3.97

[a] M and C are not adsorption sites in this work

Table 1(b) Adatom height and nearest dimer length at the corresponding sites in Table 1(a)

Site	Adatom Height (Å)[a]	Dimer Length (Å)[c]
B	1.54	3.80
A	2.27	2.47
F	1.31	2.69
D	1.92	2.48
M[a]	0.92	2.54
C[a]	1.88	2.61

[a] M and C are not adsorption sites in this work.

[b] The adatom heights are relative to the dimers on the fully relaxed clean surface.

[c] The original dimer length is 2.51 Å.

The first four sites labeled B, A, F and D correspond to local minima. Here, the global minimum occurs at site F, in agreement with previous works using MD simulation [13,14]. However, point C is found to be at the top of the barrier separating two adjacent B sites and is energetically unstable. This is in contrast to the results of Lu and Srivastava [13,14]. The former performed the total-energy minimization using the original SW potential while the latter used the Tersoff potential [29]. At the D site, the repulsive three-point term is large since the adatoms is now bonded not only to the two surface atoms but also to a third atom in the second layer. An atom at A is bonded to only one surface atom with the result that the repulsive three-point term is almost zero. As for the B site, we get a negative repulsive three-point term, indicating that a local rearrangement of surface atoms around the B site must have taken place. Indeed, Table I indicates that for all adsorption sites except B, the surface dimer is closed. However, for adsorption at site B, the dimer spontaneously opens. This phenomena has also been observed by workers using the MD simulation [14]. The bonding geometries at sites M,D, and C are shown in Fig. 2.
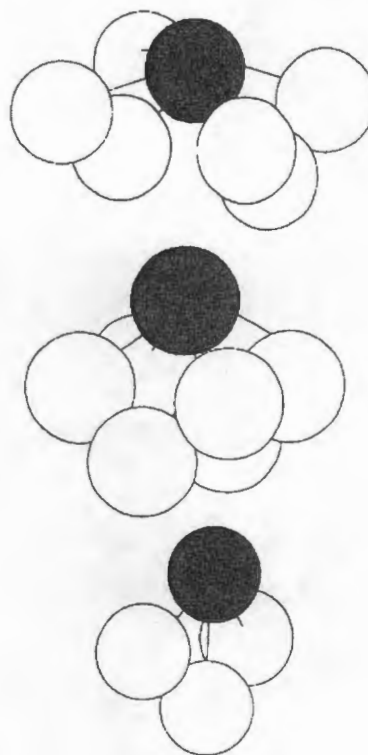

Fig. 2. The bonding geometries of an adatom at (a) site M, (b) site C and (c) site D. Note that the solid circles represent the adatoms.

We now consider the dynamics of an adatom at low temperatures (about 300 K). In Table 2, we list the various types of jumps, the corresponding jump rates, the total rate of escape from each adsorption site, the jump probabilities, and the barriers between sites. A close examination of the table reveals some kind of localization effect. If we trace the path of an atom from all sites, we can see that an atom that lands on a B or D site has a high

Table 2 Jump diffusion dynamics of a Si adatom on Si(001) - 2   x 1 surface at 300 K.

Jump Type	Jump Rate	Total Escape	Jump Probabilities	Barrier (eV)
B _ B	4.91×10^{-8}		6.14×10^{-4}	1.21
B _ D	7.59×10^{-5}	1.60×10^{-2}	1.90×10^{-2}	1.02
B _ A	7.84×10^{-3}		0.98	0.90
A _ B	1.29×10^{5}		1.88×10^{-6}	0.47
A _ D	1.38×10^{9}	6.86×10^{10}	~ 0.04	0.23
A _ F	6.58×10^{10}		~ 0.96	0.13
F _ F	4.04×10^{-20}		5.32×10^{-16}	1.93
F _ A	7.59×10^{-5}	1.52×10^{-4}	~ 1	1.02
F _ D	3.28×10^{-9}		8.63×10^{-5}	1.28
D _ A	8.92×10^{5}		~ 1	0.42
D _ B	0.81	1.79×10^{6}	9.05×10^{-7}	0.78
D _ F	1.84×10^{3}		2.06×10^{-3}	0.58

probability of jumping to a neighbouring A site. We also note that the escape rate from B is low. From A, it will most probably jump to F and remain there for a long time. Even if it manages to escape from F, it will most likely land in one of the two A sites where it will again hop back to F. Thus, B and especially F act as effective traps for the adatom, which comes as no surprise since these are the regular binding sites for ordered growth of Si on the Si(100) surface.

At higher temperatures (about 700 K), the probability of an A -> F jump is still high although now there is a finite probability of a jump to any of the two D sites (refer to Table3).

Table 3   Jump diffusion dynamics of a Si adatom on Si(001) - 2 x 1 surface at 700 K.

Jump Type	Jump Rate (sec^{-1})	Total Escape Rate (sec^{-1})	Jump Probabilities
B _ B	1.98×10^4		4.60×10^{-3}
B _ D	4.60×10^5	8.60×10^6	~ 0.21
B _ A	3.36×10^6		~ 0.79
A _ B	4.16×10^8		2.6×10^{-4}
A _ D	2.22×10^{11}	1.60×10^{12}	~ 0.28
A _ F	1.16×10^{12}		~ 0.72
F _ F	0.13		2.75×10^{-7}
F _ A	4.60×10^5	9.45×10^5	~ 0.97
F _ D	6.20×10^3		~ 0.03
D _ A	9.52×10^9		~ 0.93
D _ B	2.45×10^6	2.04×10^{10}	2.40×10^{-4}
D _ F	6.73×10^8		~0.07

We conclude that the most probable path for diffusion is as follows. A particle landing on B, F, or D will make its way to the nearest A site. From there, it will probably move to an F site although the D sites are now more accessible. Hence, we deduce that an adatom is likely to diffuse along the path D-A-D with frequent side trips to F (refer to Fig. 3).
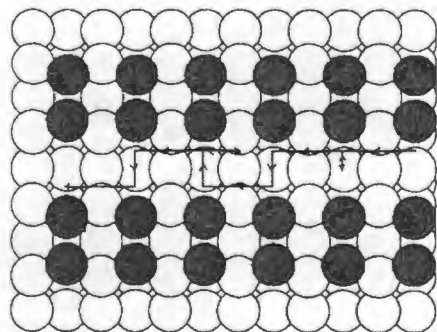

Fig. 3.   A possible path for diffusion of a Si atom on the

Si(100)-2X1 surface.   Note that the adatom may occasionally hop across a dimer row.

Lu, Zhang and Metiu [13] showed that such side trips have little effect on the effective activation energy along the main path. For our case, transition to an F site only serves to increase the lifetime of a particle at A. We also calculate an effective activation energy of 0.325 eV, which is within the range of recent experimental estimates [15,16]. Hence, we report here a first observation of the diffusion of a single Si adatom along the side of the dimer row on the Si(100)-2X1 surface.

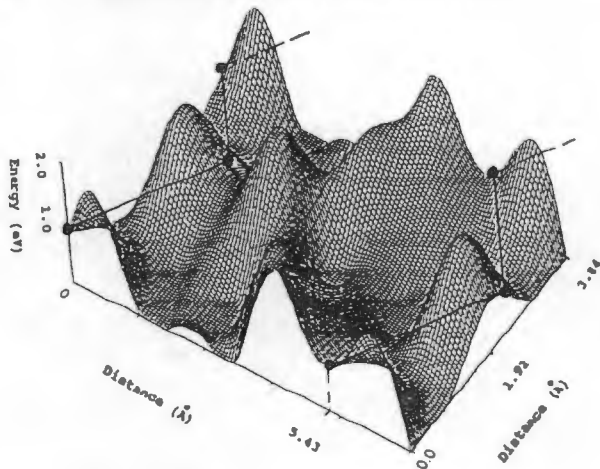B.   Adsorption on the Perfect Si(110)

Fig. 4.   The total energy surface of the Si adatom on Si(110), obtained by repeating the calculated values of the total energy within the rectangular grid ABCD in Fig. 1b throughout the surface. The dark circles represent the locations of the surface Si atoms lying on the zigzag chain.

Fig. 4 depicts the total energy surface for a Si adatom on the perfect Si(110) surface. As can be seen, a low-energy path for diffusion occurs across the plateau region, rather than in the region between the surface atomic zigzag chains as previously obtained for the diffusion of K and Al on the GaAs(110) [25] and GaP(110) [26] respectively. This low-energy path directly above a surface atomic zigzag chain (AA') is itself zigzag in nature -in fact, it is a mirror image of the surface atomic zigzag chain. The activation energy for a Si atom to diffuse along this zigzag path on the Si(110) surface is 0.054 eV, suggesting that the Si adatom can diffuse rapidly on this surface, whereas along the path AA" (a straight line connecting point A on traverse P to another symmetrical point A" on traverse P'), the barrier to diffusion is 0.19 eV (see Fig. 5).
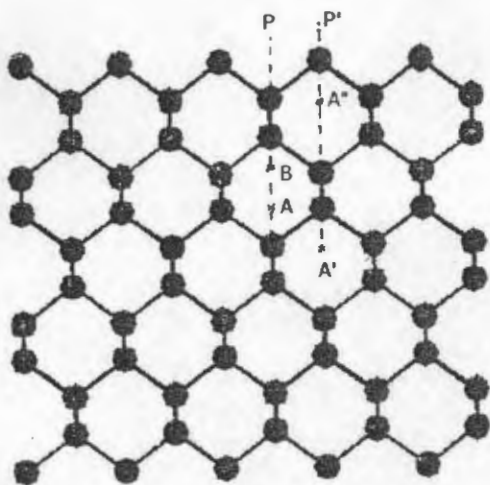
Fig. 5. Schematic illustration of the global equilibrium site of the Si adatom (site A) on traverse P and equivalent sites (sites A' and A") on neighbouring traverse P'. The diffusion barrier along path AA' is only 0.054 eV, while along AA", the barrier is 0.19 eV.

The global equilibrium binding site for a single Si adatom on Si(110) lies along traverse P at site A in Fig. 5. The binding energy of the Si adatom at site A to the surface is 3.67 eV. When the Si adatom is at the dangling bond site of one of the surface Si atoms on a zigzag chain, the binding energy is 2.63 eV. Thus, site A represents a chemisorption site for the adatom where the coordination is more than one. The height of the adatom at site A above the surface layer is 1.9 A, in good agreement with that observed by Yamamoto et al. [8] and the bulk layer separation.
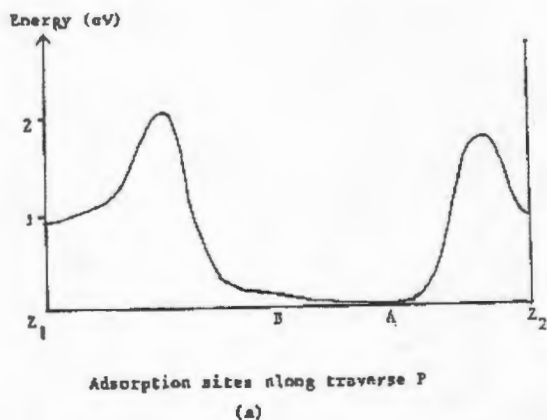

Adsorption sites along traverse P

(a)

Fig. 6a. Total energy profile of the Si adatom as it is moved along traverse P between Z_1 and Z_2 shown in Fig. 6(b).

To have a clearer picture of the adsorption profile around the vicinity of site A, Fig. 6a illustrates the total energy profile along traverse P as the Si adatom is moved from a location above a surface atomic zigzag chain to a symmetrical location above another neighbouring zigzag chain. As can be seen, there is a low energy trough between A and B (see Fig. 6b for top view of this path),
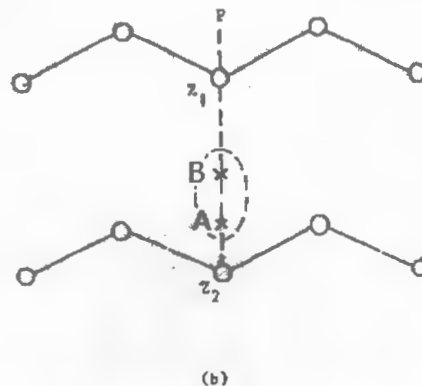

(b)

Fig. 6b. Top view of traverse P on Si(110) which illustrates a low-energy trough around the enclosed region where sites A and B are located.

with the barrier for diffusion between A and B being merely 0.12 eV. Binding sites in this low energy region between A and B is similar to the Si adatom binding site model proposed by Yamamoto et al. [8] to account for the STM observation of the spheres which are believed to be the Si adatoms on Si(110). In a recent MD (molecular dynamics) simulation of the MBE growth of Si on Si(110) [30] using the Tersoff potential [29], a threefold-coordinated site (T), similar to site B in our calculation isfound to be most stable and closest to the surface (1 A above the surface layer). However, another distinct adsorption twofold-coordinated site (M), which is similar to site A in this work, is found to be 1.6 eV higher than site T, unlike our findings where there exists a low energy path between sites A (M) and B (T). Thus, our calculations suggest that the Si adatom is quite mobile on Si(110), displaying an anisotropic diffusion along a zigzag path in the <110> direction, a mirror-image of the zigzag profile of the surface atomic zigzag chain, and also consistent with the athermal motion of its analogue in bulk Si, the self-interstitial [31].

5.   CONCLUSION

We have investigated the characteristics of the adsorption and diffusion of Si adatoms on the Si(100)-2X1 and Si(110) surfaces. Our results show that the diffusion of the Si adatom is anisotropic for both surfaces. For the Si(100) surface, the direction of easy diffusion is parallel and to the side of the dimer rows with the activation energy being about 0.33 eV. For the Si(110) surface, diffusion of the adatom is along a low-energy path directly above the surface atomic zigzag chain, with the activation energy being 0.054 eV. In addition, the height of the Si adatom above the surface is also consistent with that observed via the STM and the inter-layer separation [8].

References

(1)   A.I. Shkrebtii, C.M. Bertoni, R. Del Sole and B.A. Nesterenko, Surf. Sci. **239** 227 (1990).

(2)   H. Neddermeyer and St. Tosch, Phys. Rev. B **38** 5784 (1988).

(3) H. Ampo, S. Miura, K. Kato, Y. Ohkawa and A. Tamura, Phys. Rev. B **34** 2329 (1986).

(4) B.A. Nesterenko and A.I. Shkrebtii, Surf. Sci. **213** 309 (1989).

(5) T. Sakurai, K.C. Pandey and H.D. Hagstrum, Phys. Lett. **56A** 204 (1976).

(6) P. Martensson, G.V. Hansson and P. Chiaradia, Phys. Rev. B **31** 2581 (1985).

(7) Y. Yamamoto, S. Ino and T. Ichikawa, Jpn. J. Appl. Phys. **25** L331 (1986).

(8) Y. Yamamoto, S. Kitamura and M. Iwatsuki, Jpn. J. Appl. Phys. **31** L635 (1992).

(9) D. Haneman, Rept. Progr. Phys. **50** 1045 (1987).

(10) K.C. Pandey, Phys. Rev. Lett. **47** 1913 (1981).

(11) T. Miyazaki, H. Hiramoto and M. Okazaki, Jpn. J. Appl. Phys. **29** L1165 (1990).

(12) G. Brocks, P.J. Kelly and R. Car, Phys. Rev. Lett. **66** 1729 (1991).

(13) Y.T. Lu, Z.Y. Zhang and H. Metiu, Surf. Sci. **257** 199 (1991).

(14) D. Srivastava and B.J. Garrison, J. Chem. Phys. **95** 6885 (1991).

(15) Y.W. Mo, B.S. Swartzentruber, R. Kariotis, M.B. Webb and M.G. Lagally, Phys. Rev. Lett. **63** 2393 (1989).

(16) Y.W. Mo and M.G. Lagally, Surf. Sci. **248** 313 (1991).

(17) J.A. Pople and D.L. Beveridge, **Approximate Molecular Orbital Theory** (McGraw-Hill, New York, 1970).

(18) J.P. van der Eerden, G.Z. Liu, F. de Jong and M.J. Anders, J. Cryst. Growth **99** 106 (1990).

(19) F.H. Stillinger and T.A. Weber, Phys. Rev. B **31** 5262 (1985).

(20) A.H. Harker and S.B. Lyon, Harwell Report AERE-R8598 (1979).

(21) C.K. Ong, G.S. Khoo, K. Hattori, Y. Nakai and N. Itoh, Surf. Sci. **259** L787 (1991).

(22) N. Itoh, K. Hattori, Y. Nakai, J. Kanasaki, A. Okano, C.K. Ong and G.S. Khoo, Appl. Phys. Lett. **60** 3271 (1992).

(23) G.S. Khoo, C.K. Ong and N. Itoh, J. Phys.: Condens. Matter **5** 1187 (1993).

(24) G.S. Khoo, C.K. Ong and N. Itoh, Phys. Rev. B **47** 2031 (1993).

(25) G.S. Khoo and C.K. Ong, J. Phys.: Condens. Matter **5** 6507 (1993).

(26) G.S. Khoo and C.K. Ong, Phys. Rev. B **48** 11936 (1993).

(27) J.H Wilson, T.J. Todd and A.P. Sutton, J. Phys.: Condens. Matter **2** 10259 (1990).

(28) A.H. Harker and F.P. Larkins, J. Phys. C: Solid St. Phys. **12** 2497 (1979).

(29) J. Tersoff, Phys. Rev. B **38** 9202 (1988).

(30) M.F. Crowley, D. Srivastava and B.J. Garrison, Surf. Sci. **284** 91 (1993).

(31) P. Masri, A.H. Harker and A.M. Stoneham, J. Phys. C: Solid St. Phys. **16** L613 (1983); G.S. Khoo and C.K. Ong, J. Phys. C: Solid St. Phys. **20** 5037 (1987).